Materials Letters 65 (2011) 2341–2344

Contents lists available at ScienceDirect

Materials Letters

journal homepage: www.elsevier.com/locate/matlet

A facile one-step hydrothermal method to produce graphene–MoO_3 nanorod bundle composites

Xiaofei Yang [a,*], Chunyu Lu [a], Jieling Qin [a], Rongxian Zhang [b], Hua Tang [a], Haojie Song [a]

[a] School of Materials Science and Engineering, Jiangsu University, Zhenjiang 212013, China
[b] School of Chemistry and Chemical Engineering, Jiangsu University, Zhenjiang 212013, China

ARTICLE INFO

Article history:
Received 28 January 2011
Accepted 4 May 2011
Available online 11 May 2011

Keywords:
MoO_3
Nanorod bundles
Hydrothermal
Electron microscopy
X-ray techniques

ABSTRACT

We describe a facile *in situ* hydrothermal fabrication of graphene–MoO_3 nanorod bundle composites utilizing sodium salicylate. The structure, morphology and composition of graphen–MoO_3 composites were investigated by means of field-emission scanning electron microscopy (FE-SEM), transmission electron microscopy (TEM), X-ray diffraction (XRD), Raman spectroscopy and thermogravimetric-differential scanning calorimetry (TG-DSC). FESEM and TEM studies show that the presence of ordered MoO_3 nanorod bundles in composites, the characterization results of XRD, Raman spectra and TG-DSC analysis confirm the reduction of graphite oxide (GO) to graphene accompanying by the formation of MoO_3 nanorod bundles in the hydrothermal process. Due to characteristics of MoO_3 and graphene–MoO_3 composites, our findings may have implications in the synthesis and fabrication of well-defined functional graphene–MoO_3 hybrid materials. It may also provide a general approach for the preparation of graphene–metal oxide hybrid materials.

1. Introduction

Graphene, a rising star in carbon family, is becoming one of the most appealing candidates for the preparation of functional hybrid materials due to its high conductivity, large surface area, flexibility and chemical stability. Most recently, efforts have been made to develop graphene–metal oxide nanocomposites with different morphologies for applications in energy storage devices and optoelectronic materials. A number of graphene–metal oxide hybrids or nanocomposites have been reported so far including graphene–Fe_3O_4 [1–5], graphene–Mn_3O_4[6,7], graphene–Co_3O_4[8–12], graphene–SnO_2 [13–16], graphene–ZnO [17–21], and graphene–TiO_2[22–26], in which metal oxides are distributed onto the surface of graphene or between the graphene layers.

MoO_3 is one of the most important layered materials and n-type metal oxide semiconductors; MoO_3 nanomaterials have drawn increasing attention because of their unique properties in many fields such as photochromic and electrochromic devices, energy storage, gas sensors and catalysis. Despite the importance of MoO_3-based nanomaterials and their wide applications in various areas, the synthesis and fabrication of high-quality MoO_3–graphene nanocomposites is rare. It is highly desirable to develop new methods for economic, large-scale production of well-ordered graphene–MoO_3 nanocomposites.

Herein we report a facile *in situ* hydrothermal approach to synthesize high-quality graphene–MoO_3 nanorod bundle composites by using inexpensive organic compound sodium salicylate as the structure-directing agent. Due to characteristics of graphene–MoO_3 functional hybrid nanomaterials, our findings may have implications in the scalable synthesis of functional graphene–MoO_3 composites. It may also provide a facile approach for the preparation of well-defined graphene-transition metal oxide nanomaterials.

2. Experimental

All reagents are analytical grade and were used as received without further purification. GO was prepared by a modified Hummers' methods with additional $KMnO_4$[27]. In a typical synthesis, 20 mg of GO was dispersed in 20 mL deionized water (1 mg/mL) and bath sonicated for 1 h to give graphene oxide nanosheets. Then a solution of $Na_2MoO_4{\cdot}2H_2O$ (5.0 mmol, 1.21 g) and sodium salicylate (3.0 g) in 40 mL of deionized water was added to the above brown homogeneous GO suspension. After the mixture was gently stirred for 10 min, HCl (3 M) was added slowly into the solution with stirring to reach a pH of 2 at room temperature. The reaction solution was then transferred into a 100 mL Teflon-lined stainless steel autoclave and kept in an oven at 180 °C for 24 h. The autoclave was left to cool naturally to room temperature; the obtained precipitate was collected by centrifugation, washed several times with deionized water and absolute ethanol, and dried at 80 °C under vacuum overnight.

The morphologies of graphene–MoO_3 hybrid materials were examined by field-emission scanning electron microscopy (FESEM,

* Corresponding author. Tel.: +86 511 88790191; fax: +86 511 88791947.
E-mail address: xyang@ujs.edu.cn (X. Yang).

0167-577X/$ – see front matter © 2011 Elsevier B.V. All rights reserved.
doi:10.1016/j.matlet.2011.05.019

JEOL, JSM-7001F) and transmission electron microscopy (TEM, JEOL, JEM-2100). XRD patterns were collected on a Bruker D8 Advance X-ray diffractometer (Cu Kα radiation, $\lambda = 0.15406$ Å) in a 2θ range from 5° to 80°. Raman spectra of GO and graphene–MoO_3 nanocomposites were recorded on a DXR spectrometer using the 532 nm laser line. TG-DSC analysis of GO and graphene–MoO_3 nanocomposites were performed on a Netzsch STA 449C simultaneous thermal analyzer.

3. Results and discussion

In order to investigate the morphology of the as-prepared products, FE-SEM and TEM images of graphene–MoO_3 nanocomposites and GO were taken for comparison. Fig. 1(a) and (b)presents the representative FESEM image of MoO_3 nanorod bundles obtained in graphene–MoO_3 nanocomposites, showing the generation of regular MoO_3 nanorod bundles with different widths and lengths. Due to the presence of large quantities of MoO_3 nanorod bundles and the tiny amount of GO added, direct observations of graphene sheets in SEM are invisible. TEM images of graphene–MoO_3 nanocomposites reveal the overall morphology of MoO_3 nanorod bundles and graphene sheets; it is evident from Fig. 1(c) and (d) that the co-existence of MoO_3 nanorod bundles and graphene sheets was observed.

XRD patterns of graphene–MoO_3 nanocomposites and GO are shown in Fig. 2(a). All the identified peaks of graphene–MoO_3 nanocomposites can be assigned to α-MoO_3 (orthorhombic system, space group P*bnm*, JCPDS card no. 05-0508). The presence of three strong intensities of the (020), (040), and (060) diffraction peaks originating from the sample suggests a layer crystal structure or a highly anisotropic growth of the nanostructures. Peaks due to other phases are not identified in the sample, indicating high purity of α-MoO_3 nanorod bundles. The diffraction peak around 11.3° is assigned to GO; XRD pattern of graphene–MoO_3 nanocomposites does not show any diffraction peaks resulted from GO, indicating that graphite oxide is reduced into graphene upon hydrothermal treatment. However, due to the strong intensities of the diffraction peaks from crystalline MoO_3 nanostructures, the broad diffraction peak with low intensity around 26°, corresponding to graphene, was not observed in the XRD pattern of graphene–MoO_3 nanocomposites. Fig. 2b presents Raman spectra of GO and the graphene–MoO_3 nanocomposites. Two characteristic bands were observed in Raman spectrum of GO; 1356 cm^{-1} (D band) is attributed to the local defects/disorders and 1600 cm^{-1} (G band) can be assigned to the sp^2 graphitized structure, while the Raman spectrum of graphene–MoO_3 nanocomposites reveals that the D and G bands appear at about 1344 and 1586 cm^{-1}, respectively. The hydrothermal treatment resulted in the slight increase of the I_D/I_G ratio from 1.0 for GO to 1.14 for graphene in MoO_3–graphene hybrids, which can be explained by the formation of some new and smaller sp^2 domains during the hydrothermal process. All the results can be attributed to slight aggregation of overlapped graphene sheets after hydrothermal treatment. The Raman spectrum of graphene–MoO_3 nanocomposites also shows three sharp characteristic bands of α-MoO_3. The Raman bands at 993 cm^{-1} (A_g, ν_{as} Mo=O) and 818 cm^{-1} (A_g, ν_s Mo=O) can be assigned to the asymmetrical and symmetrical stretching vibrations of the terminal Mo=O bonds while the band at 663 cm^{-1} (B_{2g}, B_{3g}, ν_{as} O–Mo–O) is attributed to the asymmetrical stretching vibration of O–Mo–O bonds. Peaks observed in the range of 50–400 cm^{-1} correspond to various bending modes of α-MoO_3 crystal.

Fig. 3(a) shows TG-DSC curves of GO between 25 °C and 800 °C where major weight losses occurred in the range of 140–300 °C with a maximum exothermal peak of 191 °C, corresponding to CO, CO_2 and steam release. A further slow mass loss observed between 400 and 800 °C can be attributed to the removal of more stable oxygen

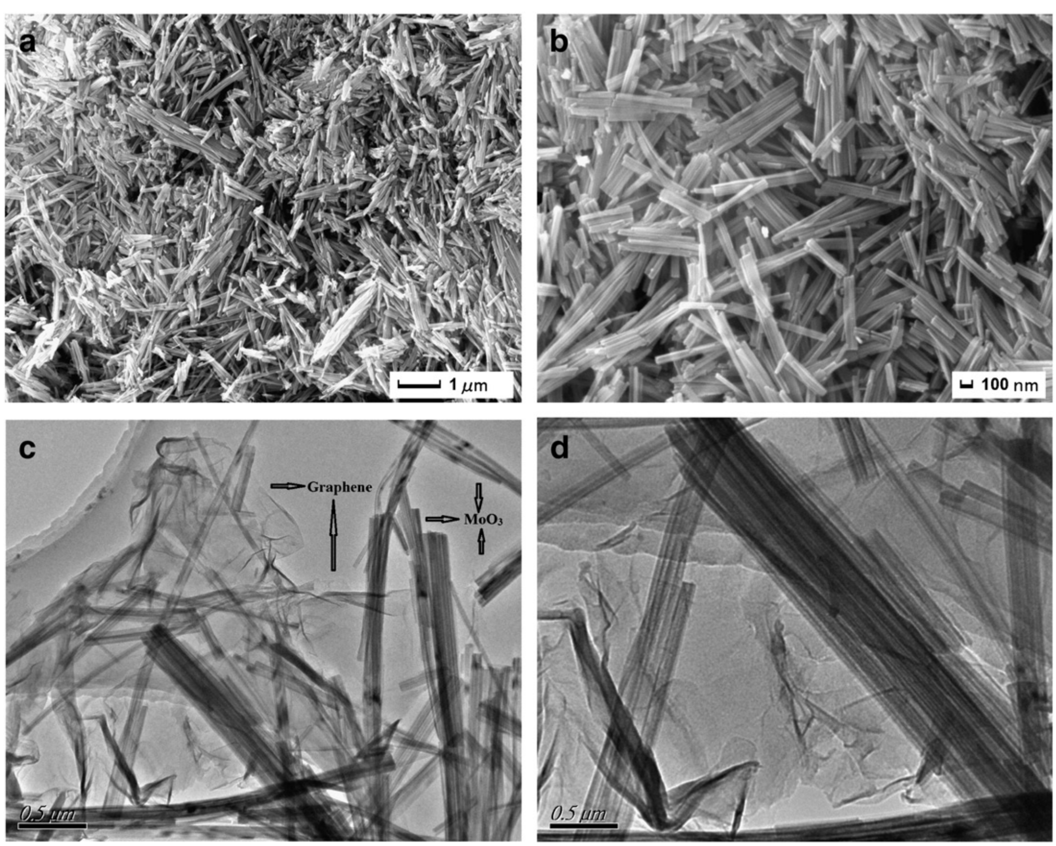

Fig. 1. FE-SEM (a and b) and TEM (c and d) observations of graphene–MoO_3 hybrids and GO. Low (a) and high magnification (b) SEM images of graphene–MoO_3 hybrids; representative TEM images of graphene–MoO_3 hybrids (c and d).